Hot-Wire Measurements of Near Wakes Behind an Oscillating Airfoil

Seung O. Park,* Jong Seong Kim,† and Boo Il Lee‡
Korea Advanced Institute of Science and Technology, Seoul, Korea

An experimental investigation was carried out to study the unsteady, near wakes behind an oscillating airfoil. The airfoil was given the harmonic pitching motion about the one-quarter chord axis at two reduced frequencies 0.1 and 0.2. The amplitude of oscillation was 7.4 deg. To assess the effect of mean incidence, the mean incidence of oscillation was varied from 0–4 deg. When the mean incidence was 4 deg, the airfoil was found to undergo a deep stall. Streamwise velocity and turbulence intensity profiles were measured by hot-wire anemometry and are presented in the paper. The near-wake measurements made it possible to detect and characterize the emergence of unsteady separation. It was found that the unsteady boundary-layer separation occurred at a greater phase angle (i.e., separation was delayed) when the reduced frequency was greater. When the mean incidence of oscillation was larger, the unsteady separation occurred at a smaller phase angle (i.e., separation was promoted). The linear relationship between the phase angle and the reduced frequency obtained in the present range of the experiment assured us that the characteristic time scale of unsteady separation was the flow time scale given by the ratio of chord length to freestream velocity. Smoke-wire flow visualization was also effected to elucidate the link between some of the measured wake data and the various flow states around the airfoil. The phase lag of wake velocity profile relative to the motion of the trailing edge was estimated. The phase lag was found to increase linearly with downstream distance except for the region very near the trailing edge.

Nomenclature

C = airfoil chord
K = reduced frequency, $\omega C/2U_\infty$
L = semiwake thickness
T = period of oscillation
t = time
U = ensemble-averaged streamwise velocity
U_e = wake-edge velocity
U_∞ = freestream velocity
u' = ensemble-averaged turbulence intensity
x = downstream distance from trailing edge
y = vertical distance from chord line
α = angle of attack
α_0 = mean incidence
α_1 = oscillation amplitude
ω = circular frequency of oscillation

Introduction

In recent years, considerable research has been conducted into the problem of unsteady aerodynamics of an oscillating airfoil. Most of previous research efforts in this area was directed to unsteady wing loading associated with dynamic stall phenomenon, as reviewed by McCroskey[1] and Carr.[2] A comprehensive review on unsteady separation over lifting surfaces has been recently given by Gad-el-Hak.[3] There are many practical situations where unsteady wakes are involved. The wake-blade interaction in turbomachinery flows is one example. Relatively scant attention, however, has been given to the study of oscillating wakes. Satyanarayana[4] measured unsteady wakes of airfoils and cascades under a sinusoidally varying gust flow. Time-mean and time-dependent wake profiles were reported in his work, and the discrepancies between these were discussed. Ho and Chen[5] studied experimentally the unsteady wake of a plunging airfoil at incidence using a hot-wire rake. The velocity traces and the Reynolds-stress distributions in their study revealed that the wake had different turbulent structures in the upper and lower parts of the wake. They also showed that the phase-averaged wake profiles are different at different phase angles. De Ruyck and Hirsch[6,7] reported the instantaneous velocity and turbulence intensity profiles of the wake of an airfoil oscillating in pitch. A trip wire was mounted over the airfoil surface to ensure turbulent flow, and a single slanted rotating wire was employed for measurements. They found hysteresis between increasing and decreasing incidences, and that turbulence levels in the unsteady case were smaller than in the corresponding static case at the same incidence. They also noticed that when the static stall limit was slightly exceeded, the wake did not appear to be stalled. Park and Kim[8] measured the wakes behind an airfoil oscillating in pitch about zero mean incidence. They observed a sudden increase in wake thickness and concluded that this was due to dynamic trailing-edge stall. The instantaneous angle of attack at which the trailing-edge stall occurred was much smaller than the static stall angle. They also found that wake thickness was increased with reduced frequency.

The primary purpose of the present study is to investigate the characteristics of the near wakes behind an airfoil oscillating in pitch with a relatively small amplitude. Hot-wire anemometry and an on-line data acquisition system were adopted to measure ensemble-averaged velocity and turbulence intensity profiles. The airfoil was given a pitching oscillation about three different mean incidences, and the resulting wakes were measured to delineate the effect of mean incidence. Data were taken for the cases of two reduced frequencies ($K = 0.1$ and 0.2) at a given combination of mean incidence and amplitude of oscillation.

Experimental Setup

The experiments were conducted in a wind tunnel of 20×30 cm cross section and test section length of 80 cm. The wind tunnel is schematically sketched in Fig. 1. An airfoil of

Presented as Paper 88-3715 at the First National Fluid Dynamics Congress, Cincinnati, Ohio, July 25–28, 1988; received Aug. 27, 1988; revision received Dec. 27, 1988. Dedicated to Professor W. R. Sears on the occasion of his 75th birthday.

*Associate Professor, Aerospace Program, Department of Mechanical Engineering. Member AIAA.

†Research Assistant, Aerospace Program, Department of Mechanical Engineering.

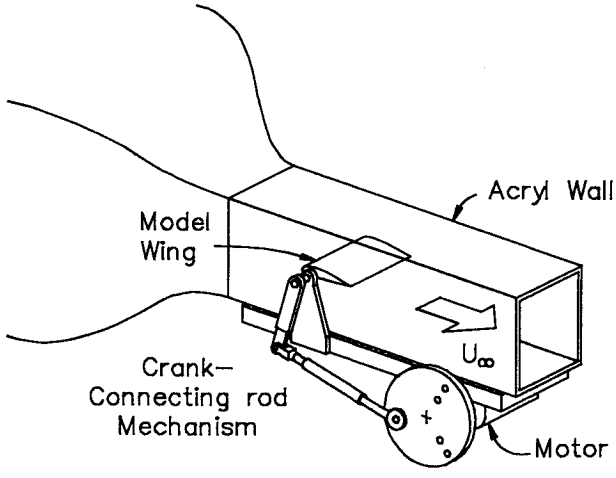

Fig. 1 Schematic of the wind tunnel.

NACA 0012 profile was mounted horizontally. The chord of the airfoil was 10 cm, and the aspect ratio was 1.98. The gap between the airfoil and the side wall was 1 mm. The ratio of the chord length to the height of the test section was 1:3, which was similar to those of previous studies[6,9]

Pitching oscillation about the quarter-chord axis was provided by a crank-connecting rod mechanism, driven by a variable-speed ac motor. The instantaneous angle of attack α can be expressed as

$$\alpha = \alpha_0 + \alpha_1 \sin\omega t \tag{1}$$

Throughout the present experiment, α_1 was set at 7.4 deg. The mean incidence α_0 was given three values: 0, 2, and 4 deg. Two values of the reduced frequency K were considered: $K = 0.1$ and 0.2. The corresponding Reynolds numbers, based on the chord length, were 4.7×10^4 and 2.7×10^4, respectively. The boundary layer developed over the airfoil surface was found to be laminar at these low Reynolds numbers.[10,11] Under these test conditions, the freestream turbulence level was 0.4%.

A DISA constant-temperature hot-wire anemometer (type 55M10) along with an I-type probe (type 55P11) were employed for the measurements. A TSI Model 1072 linearizer was used to linearize the anemometer output. The hot-wire probe was mounted on a support in the centerplane of the test section. A traversing mechanism driven by a stepping motor moved the probe support to span the wake vertically. Spatial resolution of the traversing mechanism was 0.1 mm.

To generate smoke for flow visualization, a nichrome wire of 0.1-mm diameter was installed vertically at the location of 15 mm forward of the leading edge in the centerplane of the test section. Another wire was installed spanwise over the upper surface of the airfoil at the 0.9 chordwise station from the leading edge to visualize the near surface flow. The height of the wire from the airfoil surface was 1 mm. Still photographs were taken by a 35-mm Nikon SLR camera equipped with a standard lens ($f = 1.4$). Lighting was provided by a stroboscope having a 25-μs-flash duration. The stroboscope was capable of external triggering, making it possible to take a picture at a given phase.

The use of a rather small aspect ratio wing in the present investigation deserves some comments. It may be asked whether the three dimensionality including wing-wall interaction arising from the low-aspect ratio geometry should affect the two dimensionality of the flow. Carr et al.[9] investigated the problem of two dimensionality in their experiment with a wing having an aspect ratio of 1.62. They observed that the wing-wall interaction has negligible effects when $K \geq 0.10$, contrary to the case of static-airfoil test at high angle of attack where separation is involved. In fact, the aspect ratio in the oscillating airfoil experiments reported in Refs. 6, 7, and 10 ranged from 1.6–2.1. Thus, we believe that the present experimental setup is not likely to entail any significant three-dimensional problems such as wing tip vortex-spanwise vortex interaction discussed in Gad-el-Hak and Ho.[12]

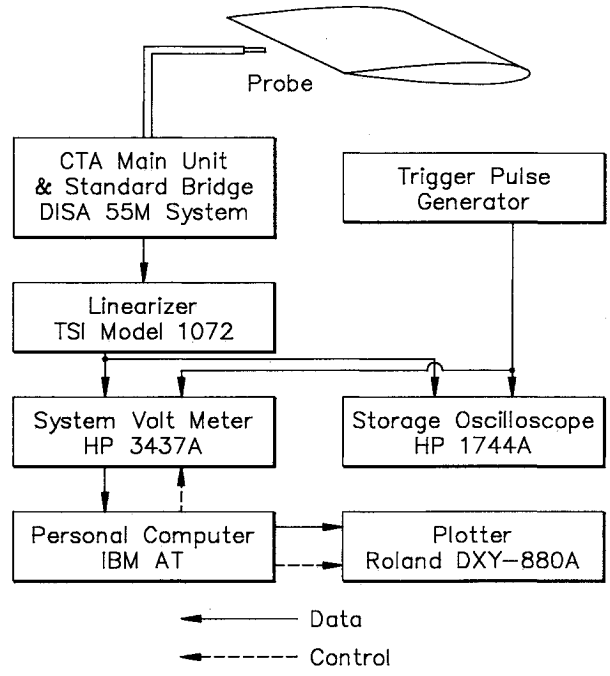

Fig. 2 Block diagram of data acquisition system.

Data Acquisition and Reduction

A reference time mark (a trigger pulse) to initiate data sampling for ensemble averaging was generated by an LED and photo-TR circuit attached to the driving disk of the crank-connecting rod mechanism. The system was adjusted to produce a trigger pulse per one revolution when the airfoil was at the mean incidence.

The block diagram for data acquisition is shown in Fig. 2. A System Voltmeter (SVM) (type HP3437A) started to operate when the trigger pulse was in. The linearized signal was digitized by the SVM, and then transferred to a personal computer (IBM AT compatible), which also processed the data. Data were taken, at a given probe location, at 48 sampling points distributed evenly over a period of oscillation. Therefore, the phase increment, $\Delta(\omega t)$ between neighboring sampling points was 7.5 deg. One hundred and fifty ensembles were used for averaging.

Measurements were carried out for four downstream stations: $x/C = 0.03$, 0.15, 0.5, and 1.0. The vertical traverse was restricted from $y/C = -0.4$ to 0.4 when the mean incidence was zero. When the mean incidence was different from zero, the range of vertical traverse was shifted downward by a small amount. For example, when the mean incidence was 2 deg, the vertical traverse ranged from $y/C = -0.43$ to 0.37. The probe was moved in increments of 1 mm for $|y/C| \leq 0.15$. Outside this range, the measurement increment was 5 mm.

When the data were reduced, it was found that some of the velocity profiles at $x/C = 0.03$ when $\alpha_0 = 4$ deg had negative velocities over a small range of angle of attack. The velocity profiles in this case exhibited double peaks when the phase angle ωt was in the range 30–45 deg, which would have been impossible without the presence of negative velocity. The velocity profiles, except for this case, did not show any double peaks at all. Thus, the measurements at $x/C = 0.03$ when $\alpha_0 = 4$ deg were somewhat inaccurate, which might have resulted in slightly larger values of wake thickness. At the

present time, the uncertainty associated with these cannot be estimated. However, comparing the various characteristics of wakes at $x/C = 0.03$ with those at further downstream stations convinced us that the qualitative observations were not affected at all by the presence of negative velocity region. Furthermore, it should be mentioned that the values of maximum turbulence intensity and the phase at which the trailing-edge stall occurs (which will be discussed later) were not influenced by the presence of negative velocity, since these were determined based on the data lying sufficiently outside of the wake centerline.

Results and Discussions

Before discussing the results of the present study, the terminology "pitch-up" or "pitch-down" to describe the state of airfoil motion is explained first to prevent confusion. The term "pitch-up" is used to describe the situation when the nose of the airfoil is moving upward and the term "pitch-down" when the nose is moving downward. Thus, when the phase angle is within the range $0 \leq \omega t \leq 90$ deg and $270 < \omega t \leq 360$ deg, the airfoil motion is described to be in "pitch-up stroke"; when $90 \leq \omega t \leq 270$ deg, the motion is said to be in "pitch-down stroke."

Velocity and Turbulence Intensity Profiles

To visualize the overall flow history of the wake, three-dimensional illustrations of velocity and turbulence intensity profiles are presented in Figs. 3 and 4, respectively. The sinusoidal "hill" of high velocity defect (Fig. 3) results from the periodic movement of the trailing edge. When $\alpha_0 = 4$ deg, a very broad region of large velocity defect is noted which is absent for the cases of $\alpha = 0$ or 2 deg. We consider that this is due to deep stall.

As seen in Fig. 4, the turbulence intensity profile variations are more complex than the velocity profiles. The high-intensity double peaks following the motion of the trailing edge are clearly visible. In addition to this, broad regions of high turbulence are noted over a certain range of instantaneous angles of attack, or t/T, as marked by "A" and "A'." We also note that these regions appear twice in a period when $\alpha_0 = 0$ and 2 deg. But, when $\alpha_0 = 4$ deg, the region appears only once. Instead, the sequential appearance of high turbulence intensity regions are notable in this case. These are marked by "A" and "B." Examination of the detailed profiles and the smoke-wire visualization pictures led us to believe that the regions marked by "A'" are due to trailing-edge stall and the region "B" is due to deep stall. Clearly, the occurrence of the

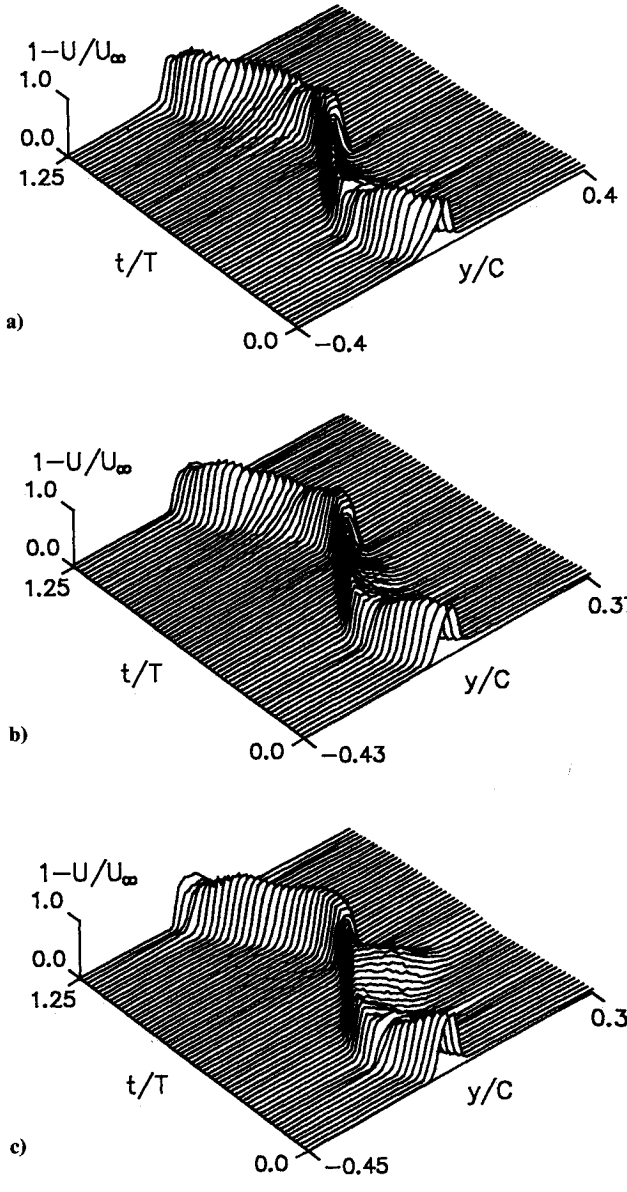

Fig. 3 Periodic variation of streamwise velocity profiles ($x/C = 0.03$, $K = 0.2$): a) $\alpha_0 = 0$ deg; b) $\alpha_0 = 2$ deg; c) $\alpha_0 = 4$ deg.

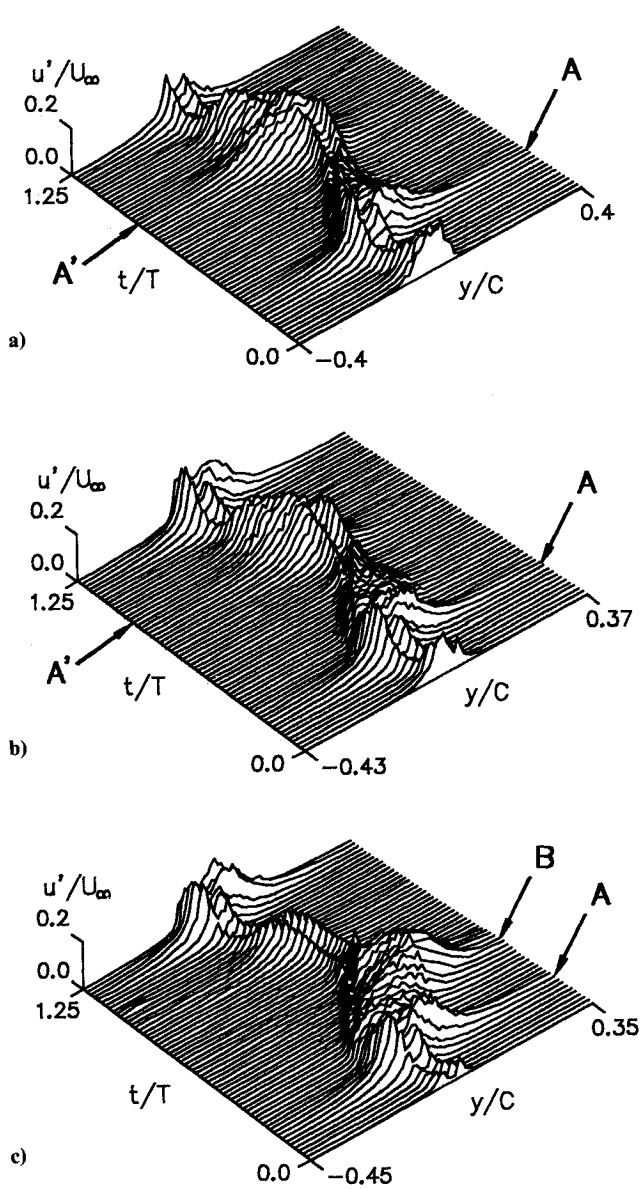

Fig. 4 Periodic variation of turbulence intensity profiles ($x/C = 0.03$, $K = 0.2$): a) $\alpha_0 = 0$ deg; b) $\alpha_0 = 2$ deg; c) $\alpha_0 = 4$ deg.

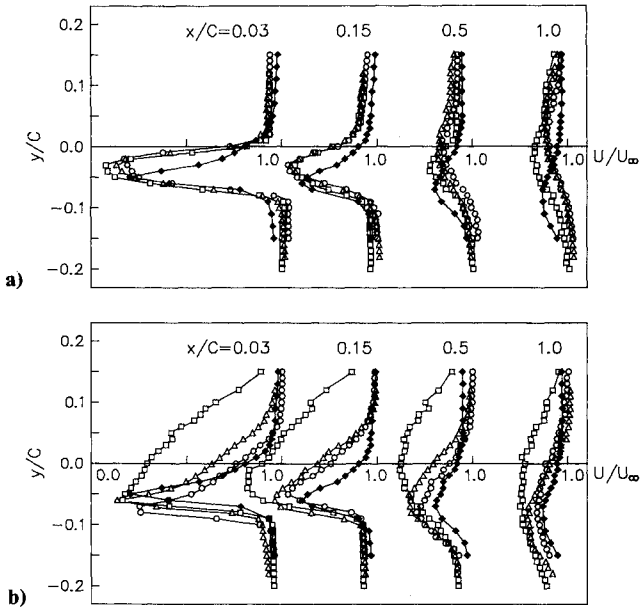

Fig. 5 Streamwise velocity profiles: a) in pitch-up stroke; and b) in pitch-down stroke at $\alpha = 4$ deg ($K = 0.2$). ○: $\alpha_0 = 0$ deg; △: $\alpha_0 = 2$ deg; □: $\alpha_0 = 4$ deg; and ◆: steady state.

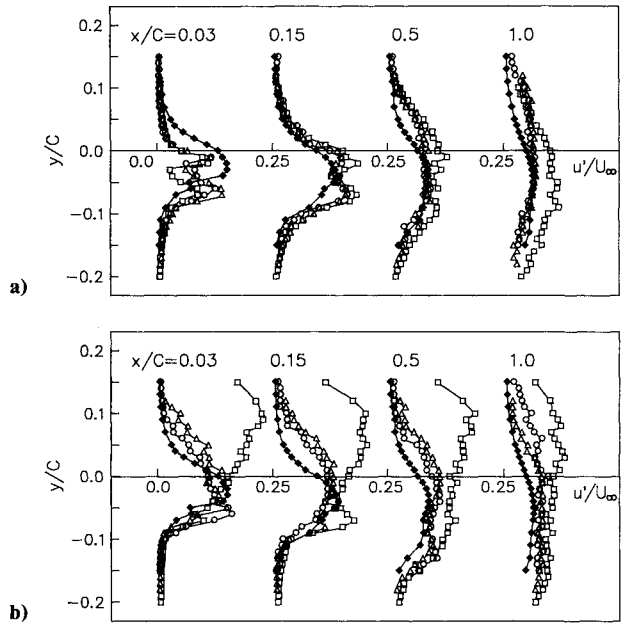

Fig. 6 Turbulence intensity profiles: a) in pitch-up stroke; and b) in pitch-down stroke at $\alpha = 4$ deg ($K = 0.2$). ○: $\alpha_0 = 0$ deg; △: $\alpha_0 = 2$ deg; □: $\alpha_0 = 4$ deg; and ◆: steady state.

region "B" is in accord with the broad region of large velocity defect of Fig. 3c.

Figures 5a and 5b illustrate streamwise velocity profiles at the instantaneous angle of attack of 4 deg in pitch-up stroke and those in pitch-down stroke, respectively. Although the instantaneous angle of attack are the same for both cases, the profiles are considerably different from each other. This clearly demonstrates the importance of time history or hysteresis of the flow.[6] In Fig. 5a, we also note that the maximum velocity-defect location tends toward the $y = 0$ axis with downstream distance. However, in Fig. 5b, the location tends away from the $y = 0$ axis. This indicates that the probe at a further downstream station detects the wake produced at a somewhat smaller angle of attack when the airfoil is in pitch-up stroke, and vice versa in pitch-downs stroke. Thus, the trend exemplified in Figs. 5a and 5b suggests that the phase lag increases with downstream distance.

The turbulence intensity profiles, corresponding to the velocity of Fig. 5, are displayed in Fig. 6. It is seen that the velocity and turbulence intensity profiles in pitch-down stroke for the case of oscillation about 4-deg mean incidence are remarkably different from the others (Figs. 5b and 6b): the wake thickness and velocity defect are much larger and the turbulence intensities are much higher. This shows that the wake in this particular case has undergone a quite different flow history than the others; the wake of the 4-deg mean incidence case in pitch-up stroke has experienced a massive separation contrary to the other two cases. See the three-dimensional illustrations of Figs. 3 and 4.

Figures 5b and 6b also suggest that the velocity defect, the wake thickness, and the turbulence intensity increase with the mean incidence. However, this trend is not obvious in the profiles of Figs. 5a and 6a, where the airfoil is in pitch-up stroke. We had closely examined the velocity and turbulence intensity profiles at various instantaneous angles of attack, and found that no conclusive statement could be drawn about the behavior of the instantaneous profiles. When the instantaneous angle of attack was -2 deg in pitch-up stroke, the turbulence level for the case of 4-deg mean incidence was of comparable magnitude to those of the other cases; at $x/C = 0.03$, it was even smaller.

Semiwake Thickness Variations

In the previous section, discussions on the velocity and turbulence intensity profiles at a given phase have been made. However, direct comparison between the profiles at a given phase can be futile because of the strong history effect involved in the flow. Thus, in this section, we examine the wake-thickness variations over a period of oscillation. As a characteristic wake thickness, the semiwake thickness defined by the distance between the two points where the mean velocity is half the velocity defect, $U_e - U_{\min}$, was selected.

Variations of semiwake thickness over a cycle of oscillation for $K = 0.2$ are depicted in Fig. 7. It is noted that the change of wake thickness for $\alpha_0 = 4$ deg is quite different from the others. The huge growth of wake thickness for $\alpha_0 = 4$ deg is considered to be a result of deep stall. When $\alpha_0 = 0$ or 2 deg, there appear somewhat smaller regions of wake thickening only in the vicinity of the maximum instantaneous angle of attack. Figure 8 illustrates how the wake thickness varies with downstream. The wake thickness representing the state of stall is seen to increase with downstream.

Stalled Flow and Visualization

As we have seen from the three-dimensional illustration of turbulence intensity variations in Fig. 4 and from the semiwake-thickness curves of Fig. 7, there exists a range of phase angle (or t/T) where the wake thickens rather abruptly. This is, of course, due to the breakdown of boundary layer over the airfoil surface. For a qualitative understanding of the boundary-layer breakdown over an oscillating airfoil surface, photographs representing some sequential flow events adjacent to the breakdown are provided in Fig. 9. The flow-visualization data contained in the figure was obtained for the case of $\alpha_0 = 0$ deg and $K = 0.2$. Plates a and b show the thin layer of reversed flow, creeping up toward the leading edge. In the subsequent "pitch-down" stroke, the layer is seen to roll up into discrete vortices. The vortical structure is then intensified and convected downstream (plates c and d). The unsteady boundary-layer separation is believed to occur somewhere between event c and d. The streakline pattern pinpointing the occurrence of unsteady separation has not been clearly understood yet. However, it is clear that the boundary layer has

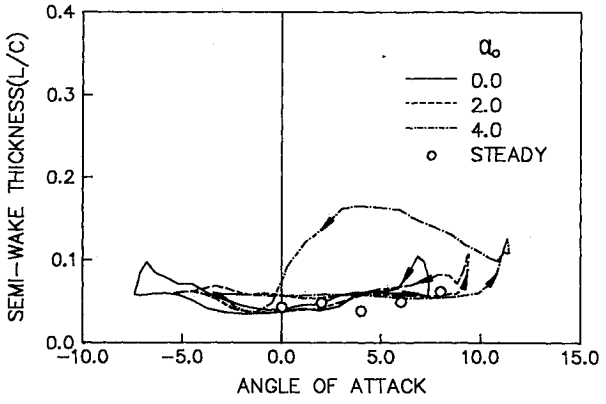

Fig. 7 Semiwake-thickness variations ($x/C = 0.03$, $K = 0.2$).

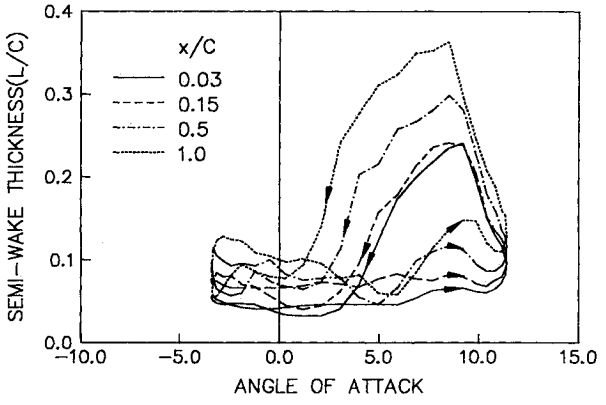

Fig. 8 Semiwake-thickness variations with downstream distance ($\alpha_0 = 4$ deg, $K = 0.1$).

been separated at the event depicted in plate d. The flow patterns observed during a cycle of oscillation are discussed in detail in Ref. 11. Since locating the exact instant of the boundary-layer breakdown is impossible by examining the wake profiles only, we select a typcial instant or phase angle which characterizes the situation. Successful selection of such an instant would enable us to clarify the relative timing of the occurrence of boundary-layer breakdown for various flow conditions. Figure 10 displays the time traces of turbulence intensity at various vertical positions at $x/C = 0.03$. Besides the intensity peaks around the locus of the trailing edge, another set of peaks is seen to be aligned at a fixed phase, which is marked by an arrow. This merely reflects that the high turbulence intensity zone is extended to a considerable height at this instant or phase. We selected this phase as a representative of the wake thickening which arises due to the boundary-layer breakdown.

The phases chosen by the criteria stated above are plotted in Fig. 11. It is seen that the phase angle increases with K, but decreases with mean incidence. Even if the phase angle decreased with the mean incidence, the instantaneous angle of attack, at which the boundary-layer breakdown was detected in the wake, was found to increase with the mean incidence. The linear relationship between the phase angle and the reduced frequency exemplified in Fig. 11 demonstrates that the proper time scale for the unsteady separation is C/U_∞, for the linear relationship results in the expression $U_\infty t/C = \text{const}$. We estimate the constant to be about 3.

Typical flow patterns related to the stalled flow are shown in Fig. 12. Also shown in the figure are the semiwake-thickness curves. The instants when the respective pictures were taken are marked in the plot. Plate a was taken prior to the instant which we had chosen to be the instant of trailing-edge stall from the turbulence profiles. Plate b was taken at the

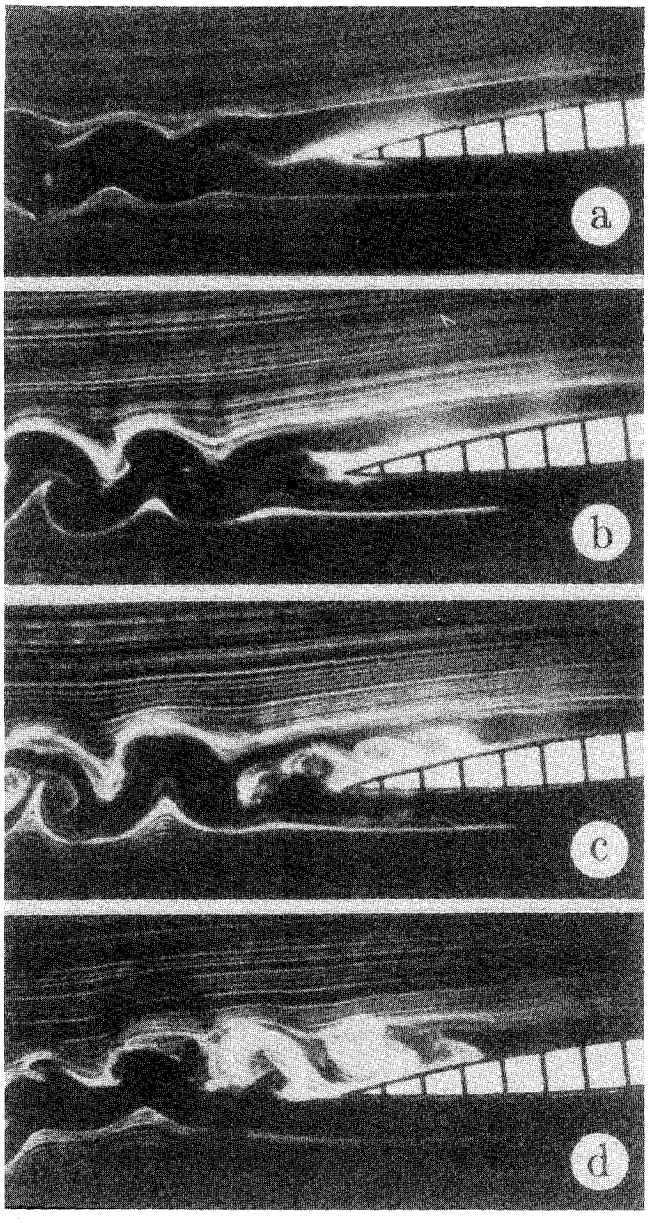

Fig. 9 Flow patterns near unsteady separation ($\alpha_0 = 0$ deg, $K = 0.2$): a) $\alpha = 6.4$ deg, $\omega t = 60$ deg; b) $\alpha = 7.4$ deg, $\omega t = 90$ deg; c) $\alpha = 7.1$ deg, $\omega t = 105$ deg; d) $\alpha = 6.4$ deg, $\omega t = 120$ deg.

instant of trailing-edge stall, and plate c was taken at an instant during deep stall. The wake visualized in plate a exhibits the characteristics of a von Karman vortex street. Also noticed are the discrete vortices formed over the upper surface of the airfoil around the trailing edge. Plate b shows that the vortices in the wake are more intensified and the wake just behind the trailing edge has become turbulent. The bright white "turbulent blob" seen over the airfoil surface is suggestive of the fact that the trailing-edge stall has occurred. From the wake-thickness curve, it is seen that the wake has thickened considerably at this instant. The wake at the instant "b" is much thicker than the one at the instant "a." The present observation is qualitatively similar to Koromilas and Telionis.[13] In their unsteady separation experiment, the abrupt thickening of the boundary layer and the appearance of a violent wake were observed. It is also recollected here that Didden and Ho,[14] in their impinging jet experiment, asserted that the ejection of the rollup vortex was associated with the onset of unsteady separation. The flow events illustrated in plates a and b support their idea. The flow pattern exhibited in plate c is very different from the other two. The

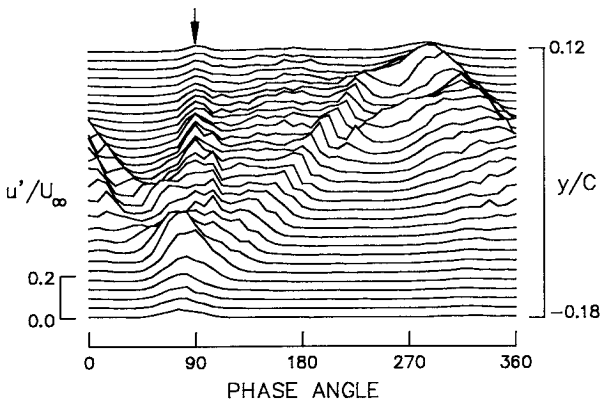

Fig. 10 Time traces of turbulence intensity at $x/C = 0.03$ ($\alpha_0 = 2$ deg, $K = 0.2$).

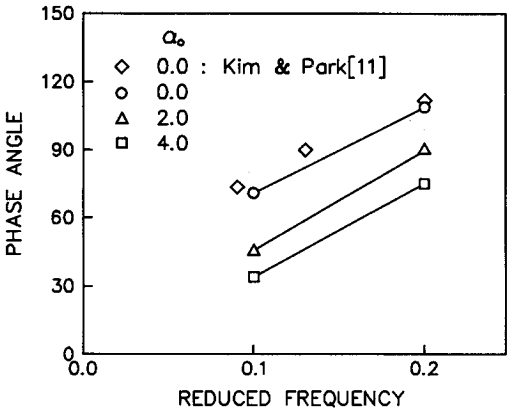

Fig. 11 Phase angle of trailing-edge stall.

wake is fully turbulent and much thicker. Virtually no smoke is seen up to a considerable height from the surface in the middle section of the airfoil. This leads us to believe that the deep stall has taken place in this case. The streakline patterns are very similar to those of dynamic stall visualized by McAlister and Carr.[10]

Phase Lag and Convection Velocity

In the wake of an airfoil, the maximum velocity-defect location is usually in line with the trailing-edge location. Therefore, if the time history of maximum velocity-defect location is known at a given downstream station, it is possible to obtain a "phase lag" relative to the motion of the trailing edge at that station. Results of such an analysis for the phase lag at several downstream stations are plotted in Fig. 13. To obtain the first harmonic of the temporal movement of the maximum velocity-defect location, we employed the direct Fourier-transform algorithm of Goertzel.[15] Figure 13 reveals that the phase lag increases linearly with downstream distance, except for the region very near the trailing edge. The linear relationship enables us to estimate the convection velocity. Since

$$(\omega \Delta t/K)/(x/C) = 2U_\infty/U_c \qquad (2)$$

where U_c is the convection velocity. Equation (2) implies that the convection velocity is independent of K. From Fig. 13, U_c was estimated to be about $0.6U_\infty$ for $0.5 < x/C < 1.5$. Carr et al.[9] showed that the traveling speed of the dynamic stall vortex over the airfoil surface was 0.35–$0.4U_\infty$. Since the degree of stall in the present experiments is much weaker than the dynamic stall, the present value of $0.6U_\infty$ seems quite reasonable.

It should be mentioned that the present analysis about the phase lag was not adequate for the flow of $\alpha_0 = 4$ deg where

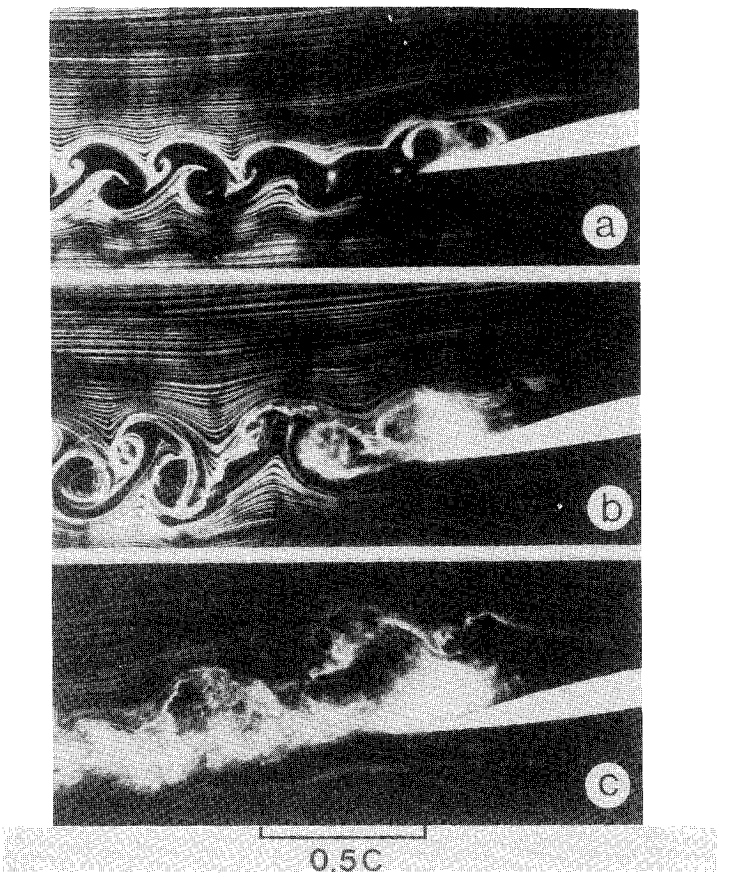

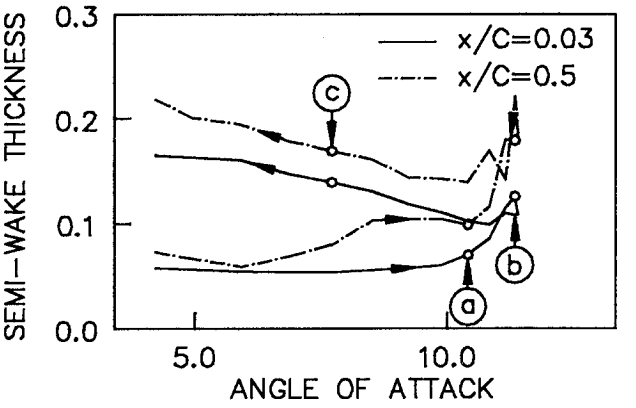

Fig. 12 Wake visualization at: a) $\alpha = 9.87$ deg, $\omega t = 52.5$ deg; b) $\alpha = 11.15$ deg, $\omega t = 75$ deg; and c) $\alpha = 8.5$ deg, $\omega t = 142.5$ deg ($\alpha_0 = 4$ deg, $K = 0.2$): flow right to left.

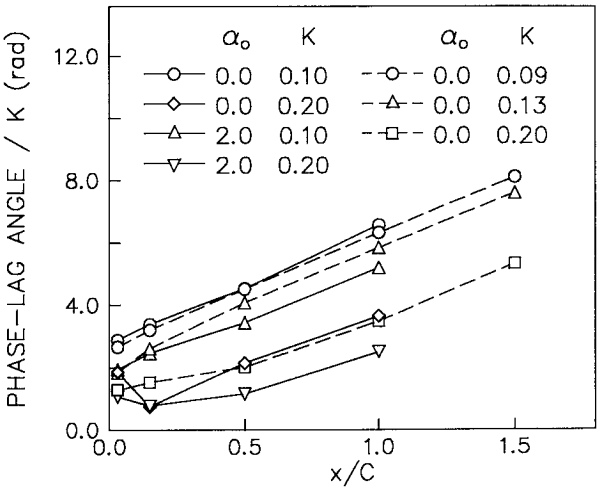

Fig. 13 Variations of phase-lag angle with downstream distance.

the maximum velocity-defect location was not well defined due to deep stall.

Conclusions

The results of the present investigation of the near wake behind an oscillating airfoil have revealed several interesting features. The ensemble-averaged mean velocity and turbulence intensity profiles were considerably different from one another even when the instantaneous angles of attack were the same. The mean velocity profile at each downstream station exhibited a phase lag relative to the periodic motion of the airfoil; the phase lag was found to increase with downstream distance. The convection velocity based on the phase lag was evaluated to be about $0.6U_\infty$.

From the wake measurements, the occurrence of trailing-edge stall could be detected. The phase at which the trailing-edge stall occurs was found to increase with the reduced frequency, but to decrease with the mean incidence.

Acknowledgments

The authors are grateful to Professor Gad-el-Hak, University of Notre Dame, and an anonymous referee for their valuable suggestions to improve the contents of the paper.

References

[1]McCroskey, W. J., "Some Current Research in Unsteady Fluid dynamics—The 1976 Freeman Scholar Lecture," *ASME Transactions, Journal of Fluids Engineering*, Vol. 99, March 1977, pp. 8–39.

[2]Carr, L. W., "Progress in Analysis and Prediction of Dynamic Stall," *Journal of Aircraft*, Vol. 25, Jan. 1988, pp. 6–17.

[3]Gad-el-Hak, M., "Unsteady Separation on Lifting Surfaces," *Applied Mechanics Review*, Vol. 40, April 1987, pp. 441–453.

[4]Satyanarayana, B., "Unsteady Wake Measurements of Airfoils and Cascades," *AIAA Journal*, Vol. 15, May 1977, pp. 613–618.

[5]Ho, C.-M. and Chen, S.-H., "Unsteady Wake of a Plunging Airfoil," *AIAA Journal*, Vol. 19, Nov. 1981, pp. 1492–1494.

[6]De Ruyck, J. and Hirsch, C., "Instantaneous Turbulence Profiles in the Wake of an Oscillating Airfoil," *AIAA Journal*, Vol. 21, May 1983, pp. 641–642.

[7]De Ruyck, J. and Hirsch, C., "Turbulence Structures in the Wake of an Oscillating Airfoil," *Unsteady Turbulent Shear Flows (Proceedings of the IUTAM Symposium on Unsteady Turbulent Shear Flows* held in Toulouse, France, on May 5–8, 1981), edited by R. Michel, J. Cousteix, and R. Houdeville, Springer-Verlag, Berlin, 1981, pp. 316–328.

[8]Park, S. O. and Kim, J. S., "Wake Measurements of an Oscillating Airfoil," *Turbulence Measurements and Flow Modeling (Proceedings of the International Symposium on Refined Flow Modeling and Turbulence Measurements* held at the University of Iowa, Iowa City, Iowa, on Sept. 16–18, 1985), edited by C. J. Chen, L.-D. Chen, and F. M. Holly, Jr., Springer-Verlag, Berlin, 1987, pp. 127–136.

[9]Carr, L. W., McAlister, K. W., and McCroskey, W. J., "Analysis of the Development of Dynamic Stall Based on Oscillating Airfoil Experiments," NASA TN D-8382, 1977.

[10]McAlister, K. W. and Carr, L. W., "Water Tunnel Visualizations of Dynamic Stall," *ASME Transactions, Journal of Fluids Engineering*, Vol. 101, Sept. 1979, pp. 376–380.

[11]Kim, J. S. and Park, S. O., "Smoke Wire Visualization of Unsteady Separation Over an Oscillating Airfoil," *AIAA Journal*, Vol. 26, Nov. 1988, 1408–1410.

[12]Gad-el-Hak, M. and Ho, C.-M., "Unsteady Vortical Flow Around Three-Dimensional Lifting Surfaces," *AIAA Journal*, Vol. 24, May 1986, pp. 713–721.

[13]Koromilas, C. A. and Telionis, D. P., "Unsteady Laminar Separation: An Experimental Study," *Journal of Fluid Mechanics*, Vol. 97, March 1980, pp. 347–384.

[14]Didden, N. and Ho, C.-M., "Unsteady Separation in a Boundary Layer Produced by an Impinging Jet," *Journal of Fluid Mechanics*, Vol. 160, Nov. 1985, pp. 235–256.

[15]Oppenheim, A. V. and Schafer, R. W., *Digital Signal Processing*, Chap. 6. Prentice-Hall, Englewood Cliffs, NJ, 1975.